International Journal of Energy Resources Applications (IJERA)
Vol. 1, Issue 1, page 40-47, 2022
https://doi.org/10.56896/IJERA.2022.1.1.006

Comparison of CFD Results of Smooth Air Duct with Experimental and Available Equations in Literature

Nitesh Dutt[1*], Abhishek Binjola[1], Ankush Jageshwar Hedau[2], Ashwani Kumar[3], Varun Pratap Singh[4], Chandan Swaroop Meena[5]
[1] Department of Mechanical Engineering,
College of Engineering Roorkee, Roorkee, Uttarakhand, India.
[2]Department of Hydro and Renewable Energy,
Indian Institute Technology Roorkee, Uttarakhand India.
[3]Technical Education Department Uttar Pradesh Kanpur, India
[4]Department of Mechanical Engineering,
School of Engineering, University of Petroleum and Energy Studies, Dehradun, India.
[5]CSIR-Central Building Research Institute, Roorkee, India, chandan@cbri.res.in
Corresponding Author: Nitesh Dutt: Email: *mech.nitesh.documents@gmail.com

Abstract

Solar air heater (SAH) has vast applications in agriculture, crop drying and other field. In solar air heater, air temperature increases at the exit section. Research has worked extensively in SAH field, experimentally and numerically to observe the performance of SAH. In the present work, a 3D model of SAH is created in Design Modeler of ANSYS and simulation is run in ANSYS Fluent for the Reynolds number range between 2000-18000. Main objective of the study is to calculate the Nusselt number (dimensionless number) and friction factor influenced by pressure drop inside the duct. Numerical results are validated with the experimental results and compared with the Modified Dittus-Boelter equation and Modified Blasius equation. Mean percentage absolute error in simulation results are within range of 10%.

Keywords: Solar Air Heater, Smooth Air Duct, CFD, 3D Model, Nusselt Number

1. Introduction

Due to the oil crisis, the high demand for energy, its availability for an extended length of time, and its fewer harmful effects on the environment and human health, renewable energy has emerged as a vital source of energy over the past few decades. Renewable energy is one of the greenest and most eco-friendly energy sources that can meet the demands of current generation. Among all the renewable, solar energy is the most prevalent, affordable, and environmentally friendly. Numerous species have survived on earth for millions of years because of solar radiations [1]. The abundance, accessibility, inexhaustibility, and cleanliness of solar energy, make it the most reliable and promising source of energy. As a renewable energy source, solar energy is completely free, very sustainable, carbon free energy source [2], [3], available all year long and can accommodate the on-going increase in energy use [4], [5] . Energy and cost bills can be greatly decreased by using solar radiation as a source of energy. Utilizing solar energy for commercial and home purposes decreases the demand for electricity for heaters and other appliances like pumping, drying, and cooking [6]. Researchers and investors are being attracted to the numerous uses of solar energy in order to

acquire efficient solar energy systems that are clean and safe for use in heating systems [7], [8]. One of the application of solar energy is SAH used for capturing solar energy and utilizing this energy for heating purpose like drying crops, seasoning wood, and heating up spaces [9] [10].

Liquid solar heaters are susceptible to a number of issues, like corrosion, fluid leakage, and energy to pump fluid. By employing air instead of liquid in solar heating equipment, all of these issues are solved [11] Main component of solar air heat is duct in which absorber plate is placed to absorb solar radiations through glass, placed at the top of duct. The air is circulated through forced convection, absorbs heat and used for space heating and other purposes [12]. However low efficiency of solar air heater may results in limited applications[13]. There are other ways to increase thermal efficiency, including multiple passage, multiple glazing, blockages, baffles, fins and obstructions, but the use of artificial repeated-rib roughness is the one that is most commonly praised and acknowledged. [11]. For enhancing effective efficiency and thermal efficiency, earlier works on SAH have used artificial roughness [10] , wire mesh, obstacle, blockages [14][15], ribs [16], phase change materials [17], duct modification, corrugated surfaces, multiple glazing passes, porous media, and other techniques [18]. Research on solar air heater is going continuously in past, however over the past ten years, there has been a rise in the usability and application of CFD based software simulations to assess the heat transfer characteristics of solar thermal systems as SAH [19]. As CFD simulation is affordable and are best suitable, when its becomes difficult to test experimentally due to time and money constraints. It is also observed that CFD results obtained are in range of acceptability of experimental results [16], [20], [21]. In the present work, a CFD simulation is represented for SAH duct having no artificial roughness (smooth duct) and results are validated with the experimental results of [22] and also with the equations available in the literature.

2. CFD Modelling and Simulation

The current work has been completed using ANSYS Fluent software, which is based on CFD. The CAD model of duct is designed in ANSYS Design Modelar, having test section dimension of 1000 mm length (l_d) , 300 mm width (w_d) and 25 mm height (h_d) . As per ASHRAY, standard test section (Fig.1) is divided into three parts, entrance section of length $5\sqrt{w_d h_d}$ (for fully develop flow), middle section is test section and the end section of length $2.5\sqrt{w_d h_d}$ [5] , where "w_d"and "h_d" are the width and height of the test section.

3. Grid or Mesh generation

Meshing of the 3D model is carried out in the ANSYS software. Coarse meshing is adopted at the entrance section, as there is no heat transfer gradient available in that section. Then fine mesh is generated in the middle (test section), because it is the main part for analysis. Then again, coarse mesh is generated in exit section. Fine meshing is done towards the absorber plate having more gradients of heat transfer. In-generated mesh, orthogonal quality is as follows: min (1), max (1), and average (1). Apart from it, minimum aspect ratio is 10.20. Figure 2 shows the mesh generated 3D duct. Fig. 3. represents the fine mesh near the absorber plate to capture the heat transfer gradients in simulation for better results.

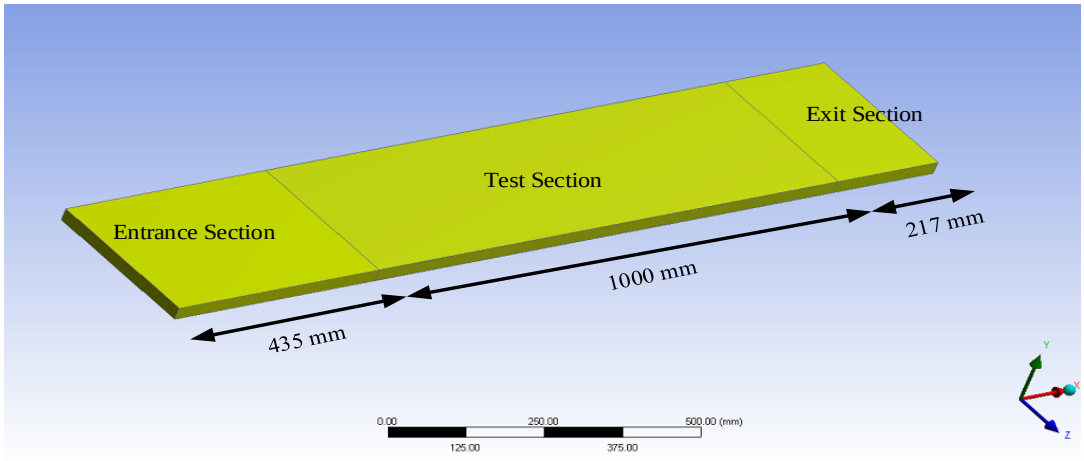

Fig. 1: Duct structure in ANSYS

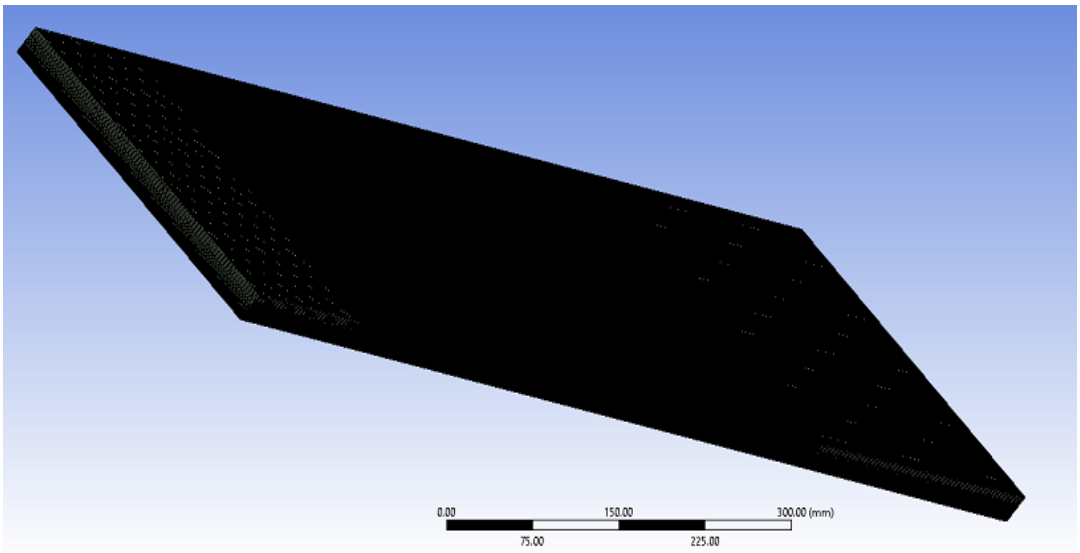

Fig. 2: Mesh generation of 3D duct

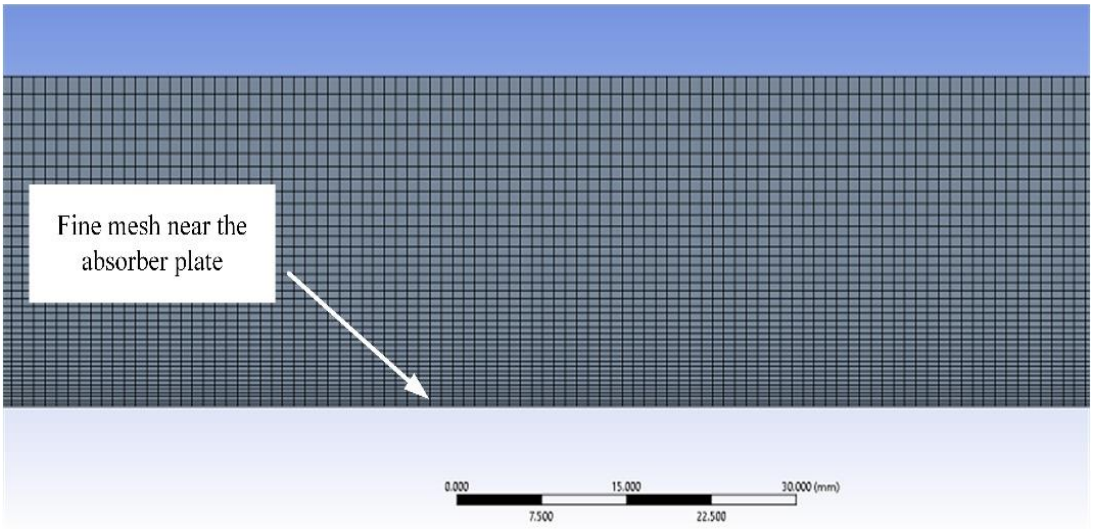

Fig.3: Fine mesh generation near the absorber plate

4. Assumptions and Boundary Conditions

Numerical simulation boundary conditions are shown in Fig. 4 and more details are mentioned are as follows:

- Absorber plate kept at the bottom of the duct having 800 W/m^2 heat flux.
- Inlet velocity for smooth duct is obtained at different Reynolds number ranges from 2000-18000.
- Air inlet temperature is taken as ambient temperature of 300 K.
- Hydraulic diameter is calculated using equation "3" is 0.0456, which is constant throughout the section.
- Outlet pressure at exit section is considered one atmosphere or zero gauge pressure.
- Adiabatic boundary condition or zero heat flux (0 W/m^2) is used at other walls of the duct.

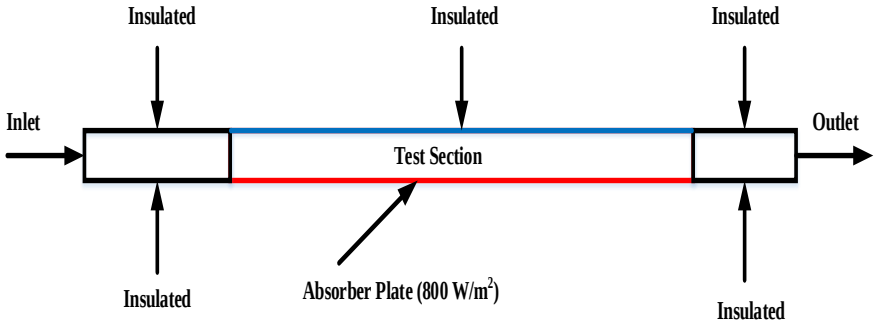

Fig. 4: Boundary condition representation

5. Results and Discussions

5.1 Solution Methods and Grid Independence Results

The governing equations in ANSYS Fluent software are solved by finite volume method. In solar air heater simulation, after modelling and meshing, Fluent setup is activated in which energy equation is activated and SIMPLE algorithm is used [12]. SST k-omega turbulence is model is selected for the simulation. Convergence criteria "none" is selected so that results are considered converged after residuals a graph becomes flat and all flux reports are balanced. In simulation, fluid domain is selected as air and constant fluid properties are taken at 300 K, as there is not so much variation in properties of air with lower temperature change. Table 1 shows the properties of air at 300 K.

Table 1: Properties of air at 300 K

Properties	Working fluid air	Unit
Thermal Conductivity (k_a) of working fluid (air) assumed constant in simulation	0.0261	(W/m.K)
Dynamic Viscosity (μ) of working fluid (air) assumed constant in simulation	0.00001853	(kg/m.s)
Specific Heat (C) of working fluid (air) assumed constant in simulation	1006.3	(J/kg.K)
Density (ρ) of working fluid (air) assumed constant in simulation	1.1765	(kg/m^3)

Table 2 shows the grid independence results in which variation in Nusselt number and friction factor is observed at Reynolds number (Re) 12000 is calculated by using equation (1)

$$\mathrm{Re} = \frac{v\rho D_h}{\mu} \tag{1}$$

The Nusselt number (Nu) is calculated using equation (2)

$$Nu = \frac{hD_h}{k_a} \tag{2}$$

Where "h" is the heat transfer coefficient having unit $\mathrm{W/m^2}.K$, "$\mathrm{D_h}$" is the hydraulic diameter, and "k_a" is the thermal conductivity of the fluid (air). Hydraulic Diameter (D_h) is calculated using the equation (3)

$$D_h = \frac{4A}{P} \tag{3}$$

In this instance, P denotes the duct perimeter "$2(w_d + h_d)$" at the test inlet and outlet of the test section. Equation (4) is used to compute the friction factor (f)

$$f = \frac{(\Delta P / l_d) D_d}{2\rho v^2} \tag{4}$$

A grid independence test is carried out by running simulation at different mesh count and variation in results is observed for friction factor and Nusselt number.

Table 2: Grid Independence Test

Sr. No.	Mesh elements generation	Value of Nusselt number (Nu)	Value of friction factor (f)	% variation in (Nu)	% variation in (f)
1	360000	44.8	0.008199		
2	3262500	42.19	0.007973	5.81	2.76
4	5381250	40.68	0.007889	3.58	1.06
4	8855000	40.19	0.007863	1.22	0.33
5	12000000	40.18	0.007863	0.03	0

5.2 Comparison of Nusselt number

The CFD results are validated with the experimental results and compared with the Modified Dittus Boelter equation. Figure 5 shows the comparative results of experimental, simulation and equation results. It has been observed that as the Reynolds number increases from 2000-18000 with a step size of 2000, the Nusselt number or heat transfer coefficient increases continuously. The reason of increase of Nusselt number is explain as follows. As the Reynolds number increases, air velocity also increases and air is more capable to carry out the heat from inlet to outlet of the duct. Further, it is observed that, Modified Dittus Boelter equation also captures the same trend. Mean absolute percentage error (MAPE) in Nusselt number (experimental vs simulation) is 6.8 %. MAPE in Nusselt number (Modified Dittus Boelter equation vs simulation) is 8.6 %.

Modified Dittus-Boelter equation for calculating Nusselt number is as follows:

$$Nu = 0.024\,\mathrm{Re}^{0.8}\,\mathrm{Pr}^{0.4} \tag{5}$$

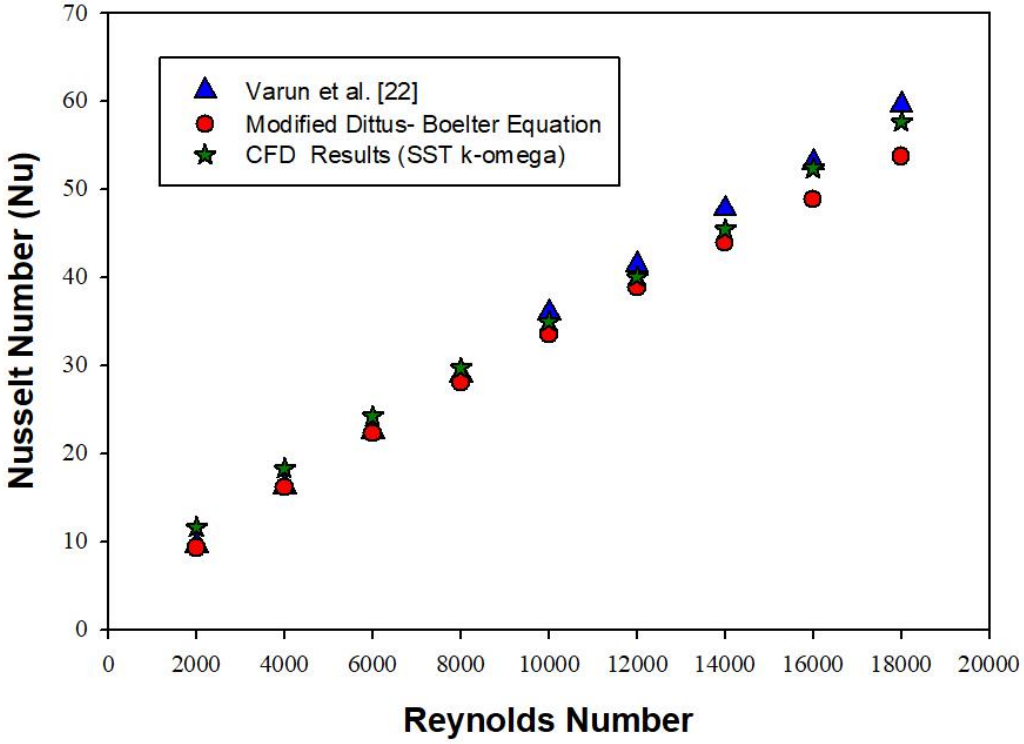

Fig. 5: Nusselt Number variation with Reynolds number

5.3 Comparison of friction factor

Friction factor details with Reynolds number are plotted in Fig. 6. In simulation results, pressure at inlet of the test section and outlet of the test section is calculated and used to find the friction factor of simulation results by using equation 4. Friction factor values are also calculated from Modern Blasius equation used in equation (6) and it is found that simulation, experimental and Modern Blasius results are in good agreement with each other.

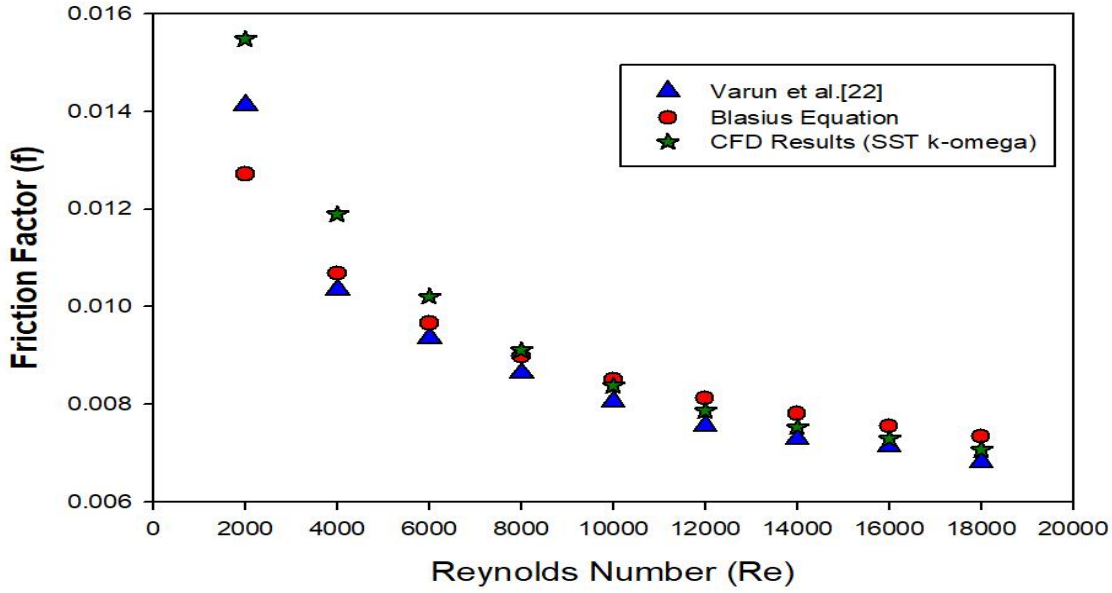

Fig. 6: Friction factor variation with Reynolds number

Modified Blasius equation for calculating friction factor is given in equation (6).

$$f_s = 0.085(Re)^{-0.25} \quad (6)$$

MAPE in friction factor (experimental vs simulation) is 6.4 %. MAPE in friction factor (Modified Blasius equation vs simulation) is 6 %.

6. Conclusion

In the present work, simulation work is carried out for Reynolds number 2000-18000, using ANSYS Fluent having SST k-omega turbulence model. Results are validated with the experimental and Modified Dittus Boelter equation for Nusselt number and Modified Blasius equation for friction factor. Mean absolute percentage error (MAPE) in Nusselt number (experimental vs simulation) is 6.8 %. MAPE in Nusselt number (Modified Dittus Boelter equation) is 8.6 %. MAPE in friction factor (experimental vs simulation) is 6.4 %. MAPE in friction factor (Modified Blasius equation vs simulation) is 6 %. Seeing the optimistic results of validation, further work can be extended for the study of heat transfer characteristics of solar air heater in which artificial roughness, baffles, ribs effects can be studied.

References

[1] R. Misra, J. Singh, S.K. Jain, S. Faujdar, M. Agrawal, A.Mishra and P.K. Goyal "Prediction of behavior of triangular solar air heater duct using V-down rib with multiple gaps and turbulence promoters as artificial roughness: A CFD analysis," *Int. J. Heat Mass Transf.*, vol. 162, p. 120376, 2020, doi: 10.1016/j.ijheatmasstransfer.2020.120376..

[2] A. Srivastava, G. K. Chhaparwal, and R. K. Sharma, "Numerical and experimental investigation of different rib roughness in a solar air heater," *Therm. Sci. Eng. Prog.*, vol. 19, p. 100576, 2020, doi: 10.1016/j.tsep.2020.100576.

[3] A. Kumar, Akshayveer, A. P. Singh, and O. P. Singh, " Efficient designs of double-pass curved solar air heaters," *Renew. Energy*, vol. 160, pp. 1105–1118, 2020, doi: 10.1016/j.renene.2020.06.115.

[4] K. Nidhul, A. K. Yadav, S. Anish, and U. C. Arunachala, "Efficient design of an artificially roughened solar air heater with semi-cylindrical side walls: CFD and exergy analysis," *Sol. Energy*, vol. 207, pp. 289–304, 2020, doi: 10.1016/j.solener.2020.06.054.

[5] K. Saurabh and H. Thakur, "Heat transfer and fluid flow analysis of artificially roughened solar air heater," *Mater. Today Proc.*, vol. 56, pp. 910–920, 2022, doi: 10.1016/j.matpr.2022.02.540.

[6] A. S. Yadav, V. Shrivastava, A. Sharma, and M. K. Dwivedi, "Numerical simulation and CFD-based correlations for artificially roughened solar air heater," *Mater. Today Proc.*, vol. 47, pp. 2685–2693, 2021, doi: 10.1016/j.matpr.2021.02.759.

[7] J. Rana, A. Silori and R. Ramola, "Numerical analysis of heat transfer and fluid flow characteristics in different V-Shaped roughness elements on the absorber plate of solar air heater duct," *International Journal of scientific & technology research* , vol.5, no. 9 ,pp.253-261.

[8] M. Al-Damook, Z. A. H. Obaid, M. Al Qubeissi, D. Dixon-Hardy, J. Cottom, and P. J. Heggs, "CFD modeling and performance evaluation of multipass solar air heaters," *Numer. Heat Transf. Part A Appl.*, vol. 76, no. 6, pp. 438–464, 2019, doi: 10.1080/10407782.2019.1637228.

[9] A. Boulemtafes-Boukadoum, R. Absi, I. El Abbassi, M. Darcherif, and A. Benzaoui, "Numerical investigation of absorber's roughness effect on heat transfer in upward solar air heaters," *Energy Procedia*, vol. 157, pp. 1089–1100, 2019, doi: 10.1016/j.egypro.2018.11.276.

[10] A. S. Yadav and J. L. Bhagoria, "A CFD based thermo-hydraulic performance analysis of an artificially roughened solar air heater having equilateral triangular sectioned rib roughness on the absorber plate," *Int. J. Heat Mass Transf.*, vol. 70, pp. 1016–1039, 2014, doi: 10.1016/j.ijheatmasstransfer.2013.11.074.

[11] V. P. Singh, S.Jain,A.Karn,A.Kumar,G.Dwivedi, C.S.Meena,N.Dutt and A.Ghosh ,"Recent Developments and Advancements in Solar Air Heaters : A Detailed Review," *Sustain.*, vol. 14, no 19, pp. 1–57, 2022, doi: 10.3390/ su141912149.

[12] S. Yadav and R. P. Saini, "Numerical investigation on the performance of a solar air heater using jet impingement with absorber plate," *Sol. Energy*, vol. 208, pp. 236–248, 2020, doi: 10.1016/j.solener.2020.07.088.

[13] V. B. Gawande, A. S. Dhoble, D. B. Zodpe and S. Chamoli, "Experimental and CFD investigation of convection heat transfer in solar air heater with reverse L-shaped ribs," *Sol. Energy*, vol. 131, pp. 275–295, 2016, doi: 10.1016/j.solener.2016.02.040.

[14] A. Bekele, M. Mishra, and S. Dutta, "Performance characteristics of solar air heater with surface mounted obstacles," *Energy Convers. Manag.*, vol. 85, pp. 603–611, 2014, doi: 10.1016/j.enconman.2014.04.079.

[15] V.P. Singh, S. Jain and A.Kumar, "Establishment of correlations for the thermo-hydraulic parameters due to perforation in a multi-V- rib roughened single pass solar air heater," *Exp. Heat Transf*, 2022, https://doi.org/10.1080/08916152.2022.2064940.

[16] I. Singh, S. Vardhan, S. Singh, and A. Singh, "Experimental and CFD analysis of solar air heater duct roughened with multiple broken transverse ribs: A comparative study," *Sol. Energy*, vol. 188, no. April, pp. 519–532, 2019, doi: 10.1016/j.solener.2019.06.022.

[17] A. Wadhawan, A. S. Dhoble, and V. B. Gawande, "Analysis of the effects of use of thermal energy storage device (TESD) in solar air heater," *Alexandria Eng. J.*, vol. 57, no. 3, pp. 1173–1183, 2018, doi: 10.1016/j.aej.2017.03.016.

[18] A. Haldar, L. Varshney, and P. Verma, "Effect of roughness parameters on performance of solar air heater having artificial wavy roughness using CFD," *Renew. Energy*, vol. 184, pp. 266–279, 2022, doi: 10.1016/j.renene.2021.11.088.

[19] H. Singh, H. Singh, and C. Kishore, "CFD numerical investigation of Heat transfer characteristics of Y- shaped solar air heater," *Mater. Today Proc.*, vol. 52, pp. 2003–2013, 2022, doi: 10.1016/j.matpr.2021.12.007.

[20] A. Kumar and A. Layek, "Nusselt number and fluid flow analysis of solar air heater having transverse circular rib roughness on absorber plate using LCT and computational technique," *Therm. Sci. Eng. Prog.*, vol. 14, p.100398, 2019, doi: 10.1016/j.tsep.2019.100398.

[21] S. Sharma, R. Singh, and B. Bhushan, "CFD based thermal efficiency of square shape protruded roughened absorber plate for solar air heater," *Energy Sources, Part A Recover. Util. Environ. Eff.*, pp. 1–22, 2021, doi: 10.1080/15567036.2021.1908460.

[22] V. P. Singh, S. Jain, and J. M. L. Gupta, "Performance assessment of double-pass parallel flow solar air heater with perforated multi-V ribs roughness — Part B," *Exp. Heat Transf.*, pp. 1–18, 2022, doi: 10.1080/08916152.2021.2019147.